Theoretical Examination of Solvent Reorganization and Nonequilibrium Solvation Effects in Microhydrated Reactions

Yoshishige Okuno*

Contribution from Research Center, Daicel Chemical Industries, Ltd., 1239 Shinzaike, Aboshi-ku, Himeji, Hyogo 671-1234 Japan

Received November 15, 1999. Revised Manuscript Received January 25, 2000

Abstract: The general features of solution reactions were clarified by theoretically investigating the following four reactions in the presence of two water molecules as solvent: (1) $NH_3 + CH_3Cl \rightarrow H_3NCH_3^+ + Cl^-$, (2) $F^- + CH_3Cl \rightarrow FCH_3 + Cl^-$, (3) $HO^- + (CH_3)_3S^+ \rightarrow HOCH_3 + (CH_3)_2S$, and (4) internal rotation in formamide. Ab initio calculations for these microhydrated reactions were used to determine the intrinsic reaction path on a solution-reaction surface that corresponds to the two-dimensional configuration space spanned by solute and solvent reactive coordinates. It was found for each reaction that the major component of the reaction-path motion in the reactant and product regions is the solvent reorganization, whereas the major reaction-path component in the transition-state region is the solute reactive motion. The solvent reorganization was shown to play a role in reducing the height of an activation barrier along the displacement of the solute reactive coordinate. Despite the moderate effect that nonequilibrium solvation was previously found to have on the contact-ion-pair formation of *t*-BuCl in the presence of four water molecules, the nonequilibrium solvation effect was found to be negligible for all the microhydrated reactions examined in the present study. This finding indicates that the solvent characterized in the transition-state region as a frozen spectator does not exert force on the solute reactive motion and that there is no simple relation between the strength of the solute−solvent interaction and the strength of the nonequilibrium solvation effect. It was also shown that the NES effect can be moderate if the motion along the intrinsic reaction path in the transition-state region comprises some solvent reactive motion. The present findings are expected to be the general features of solution reactions.

Introduction

There has been considerable theoretical interest in the mechanisms of solution reactions and in the influence of solvent reorganization on the dynamics and kinetics of these reactions. Although several studies[1−8] have explored these subjects and obtained significant insights into the reactions, these subjects are still not well understood. Several researchers have proposed several mechanisms of solution reactions,[1−3] but the studies of those researchers seem to be inadequate for determination of the mechanisms.

Kurz and Kurz[1] classified solution reactions as a coupled or an uncoupled mechanism according to whether the solute−solvent interactions are strong or weak. In the coupled mechanism, the strong solute−solvent interaction causes solvent reorganization to be synchronous with solute reactive motion. In the uncoupled mechanism, in contrast, the solvent configuration first fluctuates toward one appropriate for an imaginary intermediate structure of the solute, the solute then changes from a reactant state to a product one, and finally the solvent reorganization directs the solvent configuration to the one appropriate for the solute product state. Their classification seems, however, to be inapplicable to the determination of whether the mechanism of a given reaction is coupled or uncoupled because their classification is based on a very qualitative model.

Warshel et al.[2] considered that solution reactions follow either a solvent-driven limit, a solute-driven limit, or a concerted limit. In the solvent-driven limit, after a solvent configuration reaches the configuration appropriate for an imaginary intermediate structure of a solute, a solute-structure change *attended by a small energy change* occurs and is followed by the relaxation of the solvent configuration. In the solute-driven limit, after a reactant solute changes into a solute intermediate state, the solvent responds by moving toward an equilibrium configuration, and then the solute structure changes into the product state. The mechanism in the concerted limit is similar to the coupled mechanism of Kurz and Kurz. Although Warshel et al. examined the mechanism for a typical S_N2 reaction in aqueous solution by making trajectory calculations, they were unable to determine

* The present address: Communications Research Laboratory, Kansai Advanced Research Center, 588-2 Iwaoka Iwaoka-cho Nishi-ku, Kobe 651-2492, Japan. Fax: +81 78 969 2259. E-mail: y_okuno@crl.go.jp.

(1) Kurz, J. L.; Kurz, L. C. *J. Am. Chem. Soc.* **1972**, *94*, 4451−4461. *Isr. J. Chem.* **1985**, *26*, 339−348.

(2) Hwang, J.-K.; Creighton, S.; King, G.; Whitney, D.; Warshel, A. *J. Am. Chem. Soc.* **1988**, *110*, 5297−5311.

(3) Lee, S.; Hynes, J. T. *J. Chem. Phys.* **1988**, *88*, 6853−6862; 6863−6869. Kim, H. J.; Hynes, J. T. *J. Am. Chem. Soc.* **1992**, *114*, 10528−10537; 10508−10528. Mathis, J. R.; Kim, H. J.; Hynes, J. T. *J. Am. Chem. Soc.* **1993**, *115*, 8248−8262; Mathis, J. R.; Hynes, J. T. *J. Phys. Chem.* **1994**, *98*, 5445−5459; 5460−5470.

(4) (a) Bergsma, J. P.; Gertner, B. J.; Wilson, K. R.; Hynes, J. T. *J. Chem. Phys.* **1987**, *86*, 1356−1376. (b) Gertner, B. J.; Bergsma, J. P.; Wilson, K. R.; Lee, S.; Hynes, J. T. *J. Chem. Phys.* **1987**, *86*, 1377−1386. (c) Gertner, B. J.; Wilson, K. R.; Hynes, J. T. *J. Chem. Phys.* **1989**, *90*, 3537−3558. (d) Gertner, B. J.; Whitnell, R. M.; Wilson, K. R.; Hynes, J. T. *J. Am. Chem. Soc.* **1991**, *113*, 74−87.

(5) Tucker, S. C.; Truhlar, D. G. *J. Am. Chem. Soc.* **1990**, *112*, 3347−3361.

(6) Pollak, E. *J. Chem. Phys.* **1986**, *85*, 865−867.

(7) Okuno, Y. *J. Chem. Phys.* **1996**, *105*, 5817−5829; *Chem. Phys. Lett.* **1997**, *264*, 120−126.

(8) Sumi, H. *J. Phys. Chem.* **1991**, *95*, 3334−3350.

10.1021/ja9940221 CCC: $19.00
Published on Web 03/10/2000

whether the solution reaction corresponds to either of these limits because of the small number of their trajectories.

Hynes et al.[3] introduced dielectric continuum models and showed that the motion along the reaction path in a barrier-crossing region for each of typical S_N1 and S_N2 reactions in solution nearly coincides with a solute reactive motion in a frozen solvent environment. But, because the dielectric continuum models cannot be applied to reactions having a strong solute−solvent interaction mediated by hydrogen bonding between the solute and solvent, their examination was limited to reactions having a weak solute−solvent interaction. Therefore, whether the reaction path characterized as the solute reactive motion in the barrier-crossing region is a specific or general feature of the solution reactions has not yet been determined.

The nonequilibrium solvation (NES) effect caused by the lag of solvent reorganization in response to fast solute reactive motion has been also examined by many researchers,[4−7] but their examinations have yielded significant differences in the strength of the NES effect. Hynes et al.,[4] for example, examined the NES effect by counting the number of the barrier recrossings caused by the force the solvent exerts on the solute reactive motion. Executing molecular dynamics simulations, they showed that the NES effect is essential to the solution reactions with a strong solute−solvent interaction and that a fairly good value of the rate constant can be obtained by calculations using a frozen-solvent approximation.

Tucker and Truhlar,[5] however, examined a microsolvated reaction and suggested that the several barrier recrossings observed in the simulation studies of Hynes et al. originated not from the NES effect but from an inappropriate dividing surface between reactant and product regions. They concluded that the NES effect is negligible when the solute−solvent interaction is strong because the solvent coupled strongly with the solute responds quickly to the solute reactive motion. The difference between the conclusion of Tucker and Truhlar and that of Hynes et al. leads to the following question: Is the NES effect for solution reactions with strong solute−solvent interaction negligible or large?

To determine the general features of solution reactions and to answer this question, we used theoretical calculations to investigate four reactions, each of which is hydrated by two water molecules as solvent:

$$NH_3 + CH_3Cl \rightarrow H_3NCH_3^+ + Cl^- \quad \text{(R1)}$$

$$F^- + CH_3Cl \rightarrow FCH_3 + Cl^- \quad \text{(R2)}$$

$$HO^- + (CH_3)_3S^+ \rightarrow HOCH_3 + (CH_3)_2S \quad \text{(R3)}$$

$$\text{internal rotation in formamide } (H_2NCHO) \quad \text{(R4)}$$

We carried out ab initio calculations for these microhydrated reactions, which differ from one another in the strength of the solute−solvent interaction. In the present investigation, we used a microscopic theory,[9,10] in which a solution reaction is reduced to a simple barrier-crossing reaction on a potential-energy contour surface in the two-dimensional configuration space determined by a solute reactive coordinate and by a solvent reactive coordinate; the latter coordinate corresponds to the solvent reorganization coordinate.

Theory

The next two subsections briefly review the microscopic theory developed previously,[9,10] and the third subsection describes the explicit expression of the equation of the solute reactive motion because this expression will be useful for a comprehensive understanding of the origin of the NES effect.

Reactive Coordinates and Solution Reaction Surface. On the intrinsic reaction path (IRP)[11−13] a solute/solvent reactive coordinate[9] is defined as a signed distance along the curve that is orthogonal to the tangential plane of an equipotential energy surface in the solute/solvent coordinate space of mass-weighted Cartesians. The directions tangential to the curves are then given by the solutions of the following equations:

$$\left.\frac{d\mathbf{x}_S}{d|s^S|}\right|_{\mathbf{x}=\mathbf{x}_{IRP}} = -\left.\frac{\nabla_S V}{|\nabla_S V|}\right|_{\mathbf{x}=\mathbf{x}_{IRP}} \quad (1)$$

and

$$\left.\frac{d\mathbf{x}_B}{d|s^B|}\right|_{\mathbf{x}=\mathbf{x}_{IRP}} = -\left.\frac{\nabla_B V}{|\nabla_B V|}\right|_{\mathbf{x}=\mathbf{x}_{IRP}}, \quad (2)$$

where

$$\mathbf{x} = \begin{bmatrix} \mathbf{x}_S \\ \mathbf{x}_B \end{bmatrix} \quad (3)$$

In these equations s^S and s^B are, respectively, the solute and solvent reactive coordinates, $\mathbf{x}_S \equiv \{x_S^i\}$ and $\mathbf{x}_B \equiv \{x_B^k\}$, respectively, denote the geometries of the solute and solvent systems in the mass-weighted Cartesian coordinates, V is the Born−Oppenheimer potential energy, $\mathbf{x}_{IRP}$ denotes a point on the IRP, and ∇_S and ∇_B are $3N^S$-dimensional and $3N^B$-dimensional (N^S and N^B are, respectively, the numbers of solute and solvent atoms) gradient operators in the solute and solvent mass-weighted Cartesian coordinates. At the transition state (TS) the respective directions of the configuration changes attending the displacement of the solute and solvent reactive coordinates coincide with those of the vibrations of the solutes and solvents in the reactive normal mode (see the Appendix).

A solution-reaction surface (SRS) is defined as the two-dimensional configuration space spanned by the solute and solvent reactive coordinates (Figure 1). The IRP for the full solute−solvent space is on the SRS because the infinitesimal distance along the IRP is given by the infinitesimal displacement of the solute and solvent reactive coordinates as follows:

$$ds^2 = ds^{S^2} + ds^{B^2} \quad (4)$$

where s is the intrinsic reaction coordinate (IRC) that denotes a length measured along the IRP. Moreover, the IRP for the full solute−solvent space coincides with the IRP for the SRS because the infinitesimal motion from a point on the IRP is given by the following equation:

$$\frac{ds^S}{|\nabla_S V|} = \frac{ds^B}{|\nabla_B V|} \quad (5)$$

Therefore, examining the IRP on the SRS, one is able to determine the extent of the solvent reorganization during the course of the reaction.

Nonequilibrium Solvation Effect. The SRS description can be extended[10] to the examination of an NES effect due to the

(9) Okuno, Y. *J. Chem. Phys.* **1999**, *111*, 8034−8038.
(10) Okuno, Y. *Int. J. Quantum Chem.*, in press.
(11) Fukui, K. In *The World of Quantum Chemistry*; Daudel, R., Pullman, B., Eds.; D. Reidel: Dordrecht: Holland, 1974; pp 113−141.
(12) Fukui, K. *Acc. Chem. Res.* **1981**, *14*, 363−368.
(13) Truhlar, D. G. In *The Reaction Path in Chemistry: Current Approaches and Perspectives*; Heidrich, D., Ed.; Kluwer Academic: Dordrecht, 1995; pp 229−255.

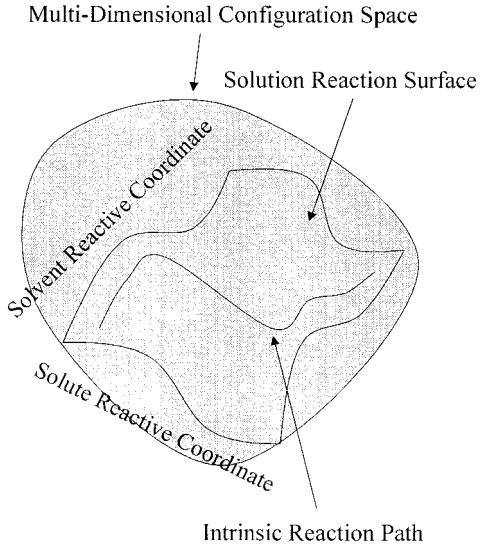

Figure 1. Schematic picture of the IRP on the SRS in a multidimensional configuration space.

lag with which the solvent reactive motion responds to the solute reactive motion. For this extension, we used a frozen model for the motions within the space spanned by the $3N^{S} + 3N^{B} - 2$ nonreactive bath modes. In this frozen model, the reactive motions are assumed to occur under the influence of a distribution static with respect to the bath modes. The frozen model for the nonreactive bath modes would give fairly good TS-region dynamics because the solute and solvent reactive motions must be faster than the nonreactive bath motions in the TS-region dynamics.

Using this frozen model, we have, as shown in ref 10, the following equations:

$$\frac{k^{na}}{k^{eq}} = \frac{\omega_S}{\omega_S^{eq}} \tag{6}$$

and

$$\frac{k^{TST}}{k^{eq}} = \frac{\lambda_S}{\omega_S^{eq}} \tag{7}$$

with the relations

$$\omega_S^{eq^2} = \omega_S^2 - \frac{g_{SB}^2}{\omega_B^2} \tag{8}$$

$$\lambda_S^2 = \frac{\omega_S^2 + \omega_B^2 - \sqrt{(\omega_S^2 - \omega_B^2)^2 + 4g_{SB}^2}}{2} \tag{9}$$

and

$$\omega_S^2 = \frac{\partial^2 V}{\partial s_0^{S^2}}, \quad g_{SB} = \frac{\partial^2 V}{\partial s_0^S \partial s_0^B}, \quad \text{and} \quad \omega_B^2 = \frac{\partial^2 V}{\partial s_0^{B^2}} \tag{10}$$

Here tangential reactive coordinates s_0^S and s_0^B denote, respectively, the distances along the directions that are tangential to the paths of the configuration changes attending the displacements of the solute and solvent reactive coordinates at the TS, k^{na} is a rate constant in a frozen solvent limit where the solvent reactive motion is assumed to be frozen in the TS region dynamics, k^{eq} is a rate constant in an equilibrium solvent limit where any configuration on the solvent reactive coordinate is assumed to adjust instantaneously to the solute reactive motion, and k^{TST} is the rate constant of the TS theory.[14] The deviation of k^{TST}/k^{eq} from unity denotes the extent of the NES effect. The agreement between the values of k^{na}/k^{eq} and those of k^{TST}/k^{eq} means that the frozen solvent approximation is appropriate to the rate-constant calculation.

Equation of Solute Reactive Motion. The force exerted by the solvent on the solute reactive motion can be represented in terms of the frictional force on the solute reactive motion. If the frozen model for the nonreactive bath modes is used, the solute reactive motion is represented by the following generalized Langevin equation:[6,15,16]

$$\begin{aligned} \ddot{s}_1^S &= -\omega_S^{eq^2} s_1^S - \int_0^t d\tau \zeta(t-\tau)\dot{s}_1^S(\tau) - R(t) \\ &= -\omega_S^{eq^2}\{s_1^S + \Gamma\int_0^t d\tau \cos\{\omega_B(t-\tau)\}\dot{s}_1^S(\tau)\} - R(t) \end{aligned} \tag{11}$$

where

$$s_1^S = s_0^S + \epsilon_S(\mathbf{Q}) \tag{12}$$

$$s_1^B = s_0^S + \epsilon_B(\mathbf{Q}) \tag{13}$$

$$\Gamma = \left(\left(\frac{g_{SB}^2}{\omega_S^2\omega_B^2}\right)^{-1} - 1\right)^{-1} \tag{14}$$

$$\zeta(t-\tau) = \frac{1}{k_B T}\langle R(t)R(\tau)\rangle \tag{15}$$

and

$$R(t) = g_{SB}\left[\left(s_1^B(0) + \frac{g_{SB}}{\omega_B^2}s_1^S(0)\right)\cos(\omega_B t) + \frac{\dot{s}_1^B(0)}{\omega_B}\sin(\omega_B t)\right] \tag{16}$$

In these equations the constants ϵ_S and ϵ_B, respectively, indicate the shifts of the equilibrium points on the solute and solvent reactive coordinates under the influence of a static distribution $\mathbf{Q}$ of the $3N^S + 3N^B - 2$ bath coordinates, k_B is the Boltzmann constant, T is the absolute temperature, t is the time, and the frictional coefficient $\zeta(t)$ denotes the magnitude of the frictional force on the solute reactive motion. Equation 11 is derived from the following system Hamiltonian given in ref 10:

$$H = \frac{1}{2}\dot{s}_1^{S^2} + \frac{1}{2}\dot{s}_1^{B^2} + \frac{1}{2}\omega_S^{eq\,2} s_1^{S^2} + \frac{1}{2}\omega_B^2\left(s_1^B + \frac{g_{SB}}{\omega_B^2}s_1^S\right)^2 + H_{bath}(\mathbf{Q},\dot{\mathbf{Q}}) \tag{17}$$

where H_{bath} is a bath Hamiltonian that depends only on the nonreactive bath coordinates and their time derivatives. According to eq 11, the influence of the frictional force on the solute reactive motion is roughly measured by the value of Γ. Therefore, when the absolute value of the solute−solvent

(14) Glasstone, S.; Laidler, K. J.; Eyring, H. *The Theory of Rate Processes*; McGraw-Hill Books: New York, 1941.

(15) Okuno, Y. Dissertation, Kyoto University, 1992. Nagaoka, M.; Okuno, Y.; Yoshida, N.; Yamabe, T. *Int. J. Quantum Chem.* **1994**, *51*, 519−527.

(16) Cortes, E.; West, B. J.; Lindenberg, K. *J. Chem. Phys.* **1985**, *82*, 2708−2717.

coupling element g_{SB} is smaller than the absolute value of the product $\omega_S\omega_B$ of vibrational frequencies for the solute and solvent reactive modes, the influence of the solvent retarding force on the kinetics of the solution reactions (i.e., the NES effect) will be small.

Method of Calculation

All the calculations were performed with the 6-31+G(d,p) basis set[17] at the Moller−Plesset second-order perturbation level of theory. For these calculations we used the Gaussian 94 program package.[17]

We first optimized the geometries for the microhydrated reactions in order to determine the relevant stationary states. For these optimizations we used a tight convergence criterion,[17] because the potential energy surfaces around the stationary states were flat; under this criterion, thresholds are to 10^{-5} au for the root-mean-square gradient and to 1.5×10^{-5} au for the maximum gradient component, and the corresponding thresholds for displacement are 4 times the gradient thresholds. The optimized geometries were identified as geometries of either stable state or TS on the basis of vibrational frequencies. We then calculated the IRC with a step length of 0.03 amu$^{1/2}$bohr by using the method of Gonzalez and Schlegel.[18] In this calculation, the optimization at a point near the stable state sometimes failed, but most of the important points on the IRP were available and these points were sufficient for examination of the characteristic of the microhydrated reactions. For the reactions R1 and R3, starting from the failed points, we also carried out rough calculations of the IRC with a larger step length and a relaxed convergence criterion for optimization and confirmed that the IRPs reach to the optimized stable structures.

We determined the IRP on the SRS by evaluating the solute and solvent reactive coordinates, which are measured from the TS, at every point on the IRP. For this evaluation, we used the value of step length for the calculation of the IRC, 0.03 amu$^{1/2}$bohr, and the energy derivatives with respect to the mass-weighted Cartesian coordinates at each nonstationary point on the IRP. At the TS the directions tangential to the directions of the configuration changes attending the displacement of the solute and solvent reactive coordinates were obtained from the vibrational vector of the unstable normal mode.

We also evaluated the rate-constant ratios k^{na}/k^{eq} and k^{TST}/k^{eq} calculated from the solute and solvent reactive frequencies ω_S and ω_B and the coupling coefficient g_{SB}. The values of ω_S, ω_B, and g_{SB} at the TS were calculated from the force constant matrix in the mass-weighted Cartesian coordinates and the relation between the mass-weighted Cartesian coordinates and the tangential reactive coordinates.

Results and Discussion

Optimized Geometries and Barrier Heights. All the optimized geometries (Figure 2) for the dihydrated Menshutkin reaction R1 were found to have cyclic structures bridged between the nucleophilic NH_3 and the leaving chlorine by two water molecules. It was also found that the ion-pair product has the chloride anion interacting directly with the amino hydrogen by hydrogen bonding. These findings are similar to those of Webb and Gordon[19] for the following Menshutkin reaction in the presence of two water molecules:

$$NH_3 + CH_3Br \rightarrow H_2NCH_3 + HBr \qquad (R1')$$

The barrier height calculated for reaction R1, 27.1 kcal/mol (Figure 2), is higher than that of reaction R1′, 24.3 kcal/mol.[19] The gradation of the barrier heights for these Menshutkin reactions coincides with that of the corresponding reaction exothermicities; the calculated energy of the product relative to that of the reactant was found to be larger for reaction R1, −13.49 kcal/mol, than for reaction R1′, −14.2 kcal/mol.[19] Therefore, the linear relationship of Evance and Polanyi between the barrier height and the reaction enthalpy[20] would hold for the series of the Menshutkin reactions.

All the optimized geometries for the dihydrated S_N2 reaction R2 were found to have cyclic structures bridged by two water molecules (Figure 2) similar to those for reaction R1. The optimized TS structure differs from that for the following S_N2 reaction in the presence of two water molecules:

$$Cl^- + CH_3Cl \rightarrow ClCH_3 + Cl^- \qquad (R2')$$

In the optimized TS structure for reaction R2′ there is no hydrogen bonding between the two water molecules.[7] This difference is due to the shorter F−Cl distance at the TS for reaction R2 than the Cl−Cl distance at the TS for the reaction R2′; the short F−Cl distance enables the two water molecules, one of which interacts with the fluorine and the other of which interacts with the chlorine, to interact with each other. The chain of the two water molecules was found to approach the leaving chlorine as the reaction proceeds. This approach is due to the shift of negative charge from the fluorine to the chlorine as the reaction progresses. The barrier height calculated for the dihydrated reaction R2, 17.3 kcal/mol, is larger than that for the corresponding gas-phase reaction, 2.61 kcal/mol.[21] The large barrier height of the dihydrated reaction is attributed to the fact that the reactant species having localized charges is significantly stabilized by the water molecules, whereas the TS species having delocalized charges is not very stabilized by the water molecules.

In all the optimized geometries (Figure 2) for the type III[20] S_N2 reaction R3 in the presence of two water molecules, both the water molecules were found to hang not on the leaving $S(CH_3)_2$ but on the oxygen of the nucleophilic OH^- (or of the product methanol). This finding can be explained in terms of the steric hindrance due to the methyl groups around the leaving S; structures similar to the bridged structures for reactions R1 and R2 must be energetically unstable. The calculated barrier height, 24.81 kcal/mol, was found to be smaller than the activation free energy of the reaction of $(CH_3)_3S^+$ with OH^- in aqueous solution, 32 kcal/mol, which was estimated from the experimental value[22] of the rate constant $k_2 = 0.133$ l/mol/h at $T = 373$ K by using the thermodynamic equation[23,24] of the TS theory:[14]

$$k_2 = \frac{k_B T}{h}\frac{RT}{P}\exp\left(-\frac{\Delta G^{\ddagger}}{RT}\right) \qquad (18)$$

where h, R, P, and $\Delta G^{\ddagger}$ are respectively the Planck constant, gas constant, pressure, and activation free energy. The number of the water molecules treated in the present study may be therefore too small to provide a quantitative result, but such a result is not essential to the present examination.

(17) Frisch, M. J.; Trucks, G. W.; Schlegel, H. B.; Gill, P. M. W.; Johnson, B. G.; Robb, M. A.; Cheeseman, J. R.; Keith, T.; Petersson, G. A.; Montgomery, J. A.; Raghavachari, K.; Al-Laham, M. A.; Zakrzewski, V. G.; Ortiz, J. V.; Foresman, J. B.; Cioslowski, J.; Stefanov, B. B.; Nanayakkara, A.; Challacombe, M.; Peng, C. Y.; Ayala, P. Y.; Chen, W.; Wong, M. W.; Andres, J. L.; Replogle, E. S.; Gomperts, R.; Martin, R. L.; Fox, D. J.; Binkley, J. S.; Defrees, D. J.; Baker, J.; Stewart, J. P.; Head-Gordon, M.; Gonzalez, C.; Pople, J. A. *Gaussian 94, Revision E.2*; Gaussian, Inc.: Pittsburgh PA, 1995.

(18) Gonzalez, C.; Schlegel, H. B. *J. Phys. Chem.* **1990**, *94*, 5523−5527.

(19) Webb, S. P.; Gordon, M. S. *J. Phys. Chem. A* **1999**, *103*, 1265−1273.

(20) March, J. *Advanced Organic Chemistry*, 4th ed.; John Wiley & Sons: New York, 1992.

(21) Wang, H.; Hase, W. L. *J. Am. Chem. Soc.* **1997**, *119*, 3093−3102.

(22) Gleave, J. L.; Hughes, E. D.; Ingold, C. K. *J. Chem. Soc.* **1935**, 236−244.

(23) Daudel, R.; Leroy, G.; Peeters, D.; Sana, M. *Quantum Chemistry*; John Wiley & Sons: Chichester, 1983.

(24) Okuno, Y. *Chem. Eur. J.* **1997**, *3*, 212−217.

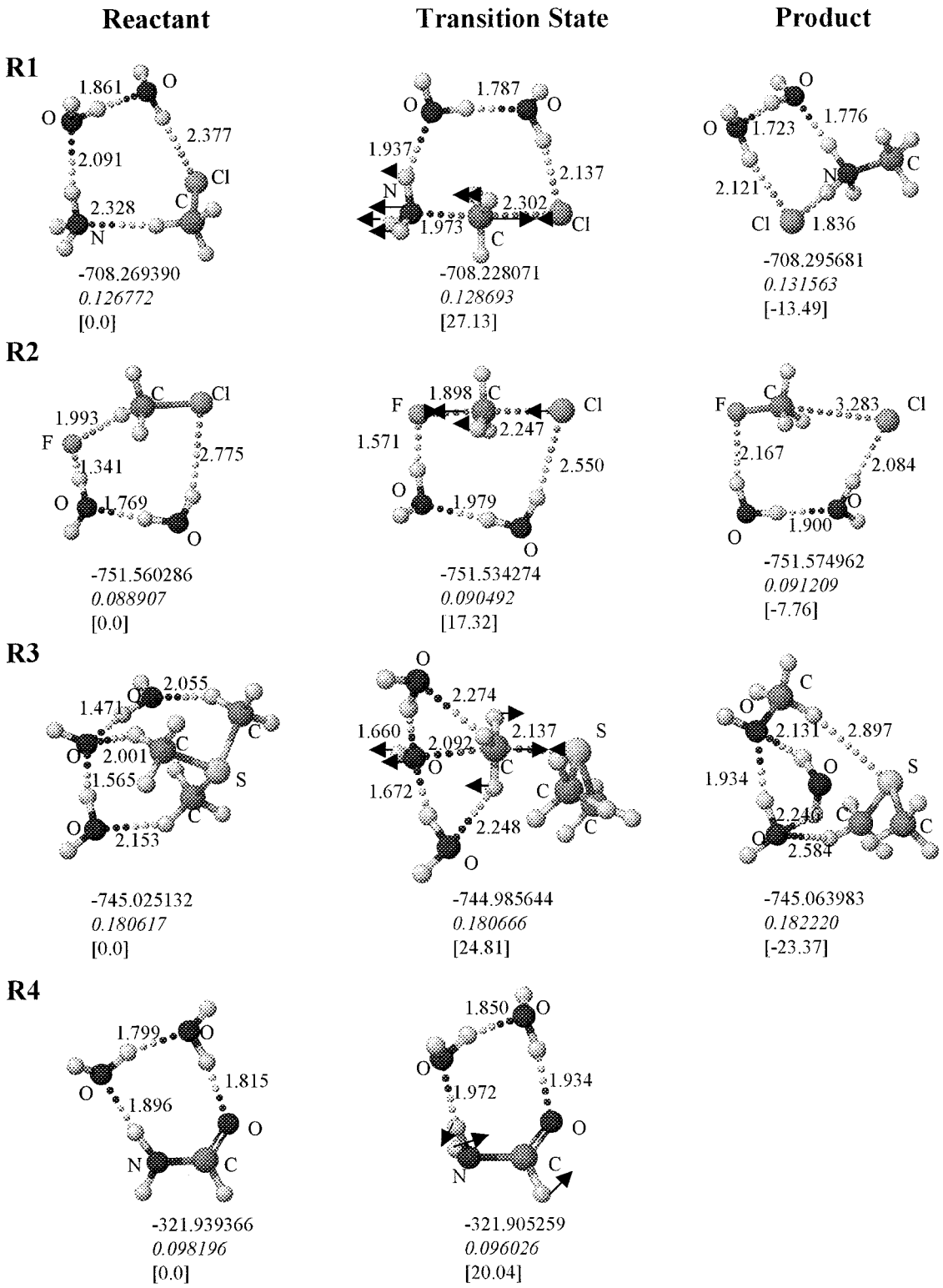

Figure 2. Optimized geometries and the total energies (in hartree) for reactions R1−R4 in the presence of two water molecules. The values in italics are zero-point energies in hartree, and the values in brackets are the relative energies with respect to the reactant species in kcal/mol. The arrows indicate the vector in the unstable normal mode at each TS.

For the internal rotation in formamide (R4) in the presence of two water molecules, the optimized geometries (Figure 2) were found to be similar to those of Chen and Gordon.[25] As they pointed out, the asymmetry of the energy profile along the displacement of the IRC (Figure 3) can be attributed to the hydrogen-bonding being temporarily lost as the TS becomes products, whereas no hydrogen-bonding is lost as the reactants form the TS. The calculated energy barrier, 20.04 kcal/mol, is also in good agreement with the 20.4 kcal/mol obtained by Chen and Gordon.

For each of the microhydrated reactions, two waters were found to interact with the solute at all the points on the IRP. This situation is not necessarily a peculiar one in the solution reactions. For example, the molecular dynamics simulations in solution[26] have shown that cyclic or cage structures around

(25) Chen, W.; Gordon, M. S. *J. Chem. Phys.* **1996**, *105*, 11081−11090.

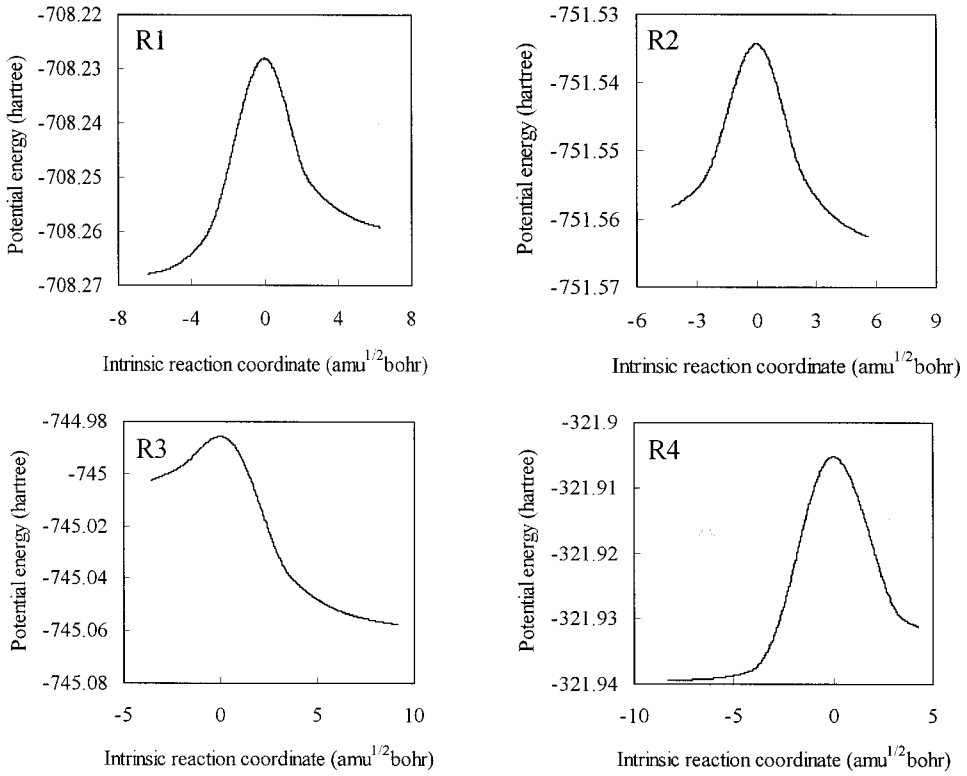

Figure 3. Potential energy profile along the displacement of the IRC for the dihydrated reactions R1−R4.

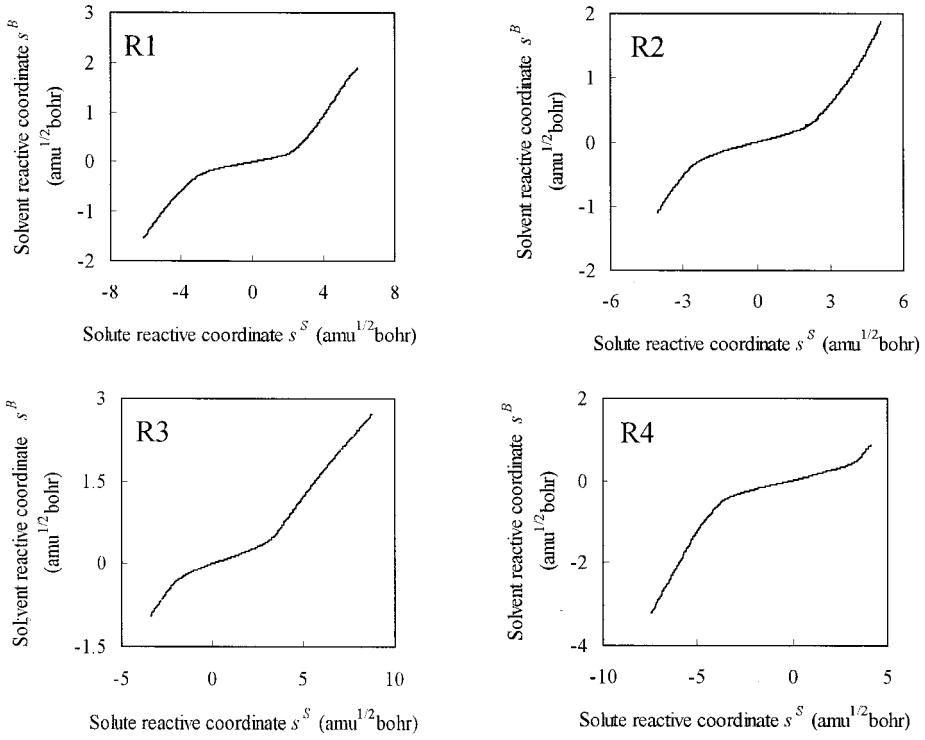

Figure 4. IRP on the SRS for the dihydrated reactions R1−R4.

solutes tend to be retained for a long time. It has been also found that the barrier crossing for the solution reaction finishes rather short time, although the vibrational relaxation takes a long time;[4d,27] thus, the solvent molecules linking by hydrogen-bonding with the solutes are expected not to exchange with any of the other solvent molecules during the barrier crossing.

(26) e.g., see, Brugé, F.; Bernasconi, M.; Parrinello, M. *J. Am. Chem. Soc.* **1999**, *121*, 10883−10888.

(27) Nagaoka, M.; Okuno, Y.; Yamabe, T. *J. Phys. Chem.* **1994**, *98*, 12506−12515.

Solvent Reorganization. It was found that the features of the IRPs on the SRSs are similar for all the microhydrated reactions examined (Figure 4). For each reaction, solvent reorganization is essential to the initial and final stages, but no solvent reorganization occurs in the region near the TS (See also unstable normal mode vectors shown in Figure 2). That is, there are three steps in all the microhydrated reactions: a first step in which there is solvent reorganization, a second step in which the configuration of the solute changes, and a third step

in which there is another solvent reorganization. This three-step mechanism had been also found previously[9] for the contact-ion-pair (CIP) formation of *t*-BuCl in the presence of four water molecules. It should be emphasized that this kind of three-step mechanism is characteristic not only of reactions with strong solute−solvent interaction but also of reactions with weak solute−solvent interaction. The three-step mechanism thus seems to be a general feature of solution reactions.

The present finding that even reactions in which the solute−solvent interaction is strong proceed by a three-step mechanism differs from the prediction of Kurz and Kurz.[1] They had thought that the strength of the solute−solvent interaction must be paramount in determining the mechanism of the solution reactions, and strong solute−solvent interaction would result in a coupled (or concerted) mechanism. Thus the difference between our finding and the prediction of Kurz and Kurz will be attributed to the fact that the mechanism of the solution reactions depends not only on the interaction strength but also on the other factors such as an inherent barrier height.

It was found that most of the barrier height for all of the microhydrated reactions comes from the energy change attending the displacement of the solute reactive coordinate and that the energy change attending the solvent reorganization occurrence is small (see Figures 3 and 4). The major role of the initial solvent reorganization is to reduce the height of the activation barrier along the displacement of the solute reactive coordinate and to facilitate the subsequent solute-configuration change. This role differs from the role of solvent reorganization in the solvent-driven limit proposed by Warshel et al.[2] They had considered that in the solvent-driven limit a large energy change attends the solvent reorganization, whereas an activation barrier along the displacement of the solute reactive coordinate is small. Although the mechanism in the solvent-driven limit may appear to be similar to the present three-step mechanism, between the present mechanism and the mechanism in the solvent-driven limit there is an essential difference in the function of the solvent reorganization.

We emphasize that the separation of solute and solvent reactive coordinates in the IRP will not be artificial, because the displacements of the solute and solvent reactive coordinates describe the solute and solvent configuration changes along the IRP, respectively. In addition, the configuration changes along the displacements of the other bath coordinates from a given point on the IRP tend to be forced back by the potential energy increase because the vibrational frequencies of the bath modes are usually real numbers. In fact, calculating the vibrational frequencies of these bath modes[10] for the reaction R2, we found that all the frequencies are always real numbers at all the points on the IRP. Thus the analysis of the IRP on the SRS will provide a significant insight into the solution reactions.

We also note that the analysis of the IRP has been widely recognized to provide qualitatively a significant insight into the chemical reaction, although the quantitative information coming from the IRP may differ from the one coming from dynamic reactive trajectories. In fact, the qualitative features we obtained are comparable with those obtained by the molecular dynamics simulations,[4d] in which a major portion of the solvent reorganization to a state appropriate to solvating the solute charge distribution at the TS was shown to take place before the charge redistribution begins.

Nonequilibrium Solvation Effect. The rate-constant ratios k^{na}/k^{eq} and k^{TST}/k^{eq} for all the microhydrated reactions were nearly 1.0 (Table 1). This indicates that the NES effect on the kinetics of all these reactions is negligible whether the solute−solvent interaction is strong or weak. The present result that even a strong solute−solvent interaction does not necessarily cause the NES effect differs from that of Hynes et al.,[4] who showed that a strong solute−solvent interaction led to a large NES effect. This difference can be attributed to the use of an inappropriate dividing surface by Hynes et al. in their calculation of a rate constant. As discussed by Tucker and Truhlar,[5] the use of an inappropriate dividing surface results in an overestimation of the number of recrossings due to the NES effect. The importance of using an appropriate dividing surface if the rate constant is to be calculated accurately has been discussed elsewhere.[28]

Table 1. Rate-Constant Ratios

reaction	k^{na}/k^{eq}	k^{TST}/k^{eq}
R1	0.99	1.00
R2	0.97	0.99
R3	0.97	0.99
R4	0.97	0.98
CIP formation[a]	0.63	0.86

[a] Values, from ref 10, for the CIP formation of *t*-BuCl in the presence of four water molecules.

Table 2. Calculated Frequencies and Coupling Elements (in cm^{-1}) and $g_{SB}^2/\omega_S^2\omega_B^2$ Ratios

reaction	ω_S	ω_B	$g_{SB}^{1/2}$	ω_S^{eq}	λ_S	λ_B	$g_{SB}^2/\omega_S^2\omega_B^2$
R1	602*i*	782	251*i*	608i	606*i*	785	−0.0179
R2	549*i*	972	353*i*	564*i*	560*i*	978	−0.0545
R3	553*i*	845	344*i*	571*i*	565*i*	853	−0.0641
R4	503*i*	390	216*i*	518*i*	509*i*	396	−0.0566
CIP formation[a]	101*i*	161	141*i*	160*i*	138*i*	186	−1.495

[a] Values, from ref 10, for the CIP formation of *t*-BuCl in the presence of four water molecules.

The NES effect is negligible for the microhydrated reactions because solvent characterized as a frozen spectator in the TS region on the reaction path does not exert force on the solute reactive motion. This can be understood through an examination of the equation of the solute reactive motion, eq 11, in which the force the solvent exerts on the solute reactive motion takes the form of a frictional force. When the motion along the IRP in the TS region is characterized as the solvent reactive motion in a frozen-solvent environment, the absolute value of the coupling element g_{SB} must be small. Then the force exerted on the solute reactive motion by the solvent, which is dependent on the value of Γ as shown in eq 14, will be negligible. The NES effect, which is caused by the solvent retarding the solute reactive motion, will consequently be negligible. In fact, the absolute values of $g_{SB}^2/\omega_S^2\omega_B^2$ for all the microhydrated reactions examined in the present study were found to be small (Table 2).

In contrast to the negligible NES effect in the microhydrated reactions examined here, there is a moderate NES effect in the CIP formation of *t*-BuCl in the presence of four water molecules (Table 1).[10,29] It had also been found[10] that the use of a frozen solvent approximation in calculating the rate constant overestimates the NES effect in the CIP formation because it neglects some adjustment of the solvent configuration to the solute reactive motion through the strong solute−solvent interaction. This solvent adjustment, however, does not necessarily lead to a negligible NES effect because the solvent cannot adjust completely to the fast solute reactive motion even through the strong solute−solvent interaction. The strength of the NES effect

(28) Okuno, Y. *J. Chem. Phys.* **1999**, *110*, 2778−2784. *Int. J. Quantum Chem.* **1998**, *68*, 261−271.

(29) Okuno, Y. *J. Phys. Chem. A* **1999**, *103*, 190−196.

in solution reactions therefore cannot be determined only by the strength of the solute−solvent interaction.

The reason that the NES effect in the CIP formation is moderate is that the motion along the IRP in the TS region comprises some solvent reactive motion through the strong solute−solvent interaction, whereas the solute reactive motion is still major component of the reaction-path motion. The contribution of some solvent reactive motion to the motion along the IRP means that in the TS region not only the solute reactive motion but also some solvent reactive motion is essential to the reaction. If the solvent reactive motion is slow compared with the solute reactive motion, the NES effect must be large. In fact, for the CIP formation, the absolute value of the coupling element g_{SB} is large compared with the absolute value of the product $\omega_S\omega_B$ of the vibrational frequencies for the solute and solvent reactive modes (Table 2). The large value of g_{SB} leads not only to the reaction-path motion represented by the synchronous change of both the solute and solvent reactive motions but also to the moderate NES effect. Tucker and Truhlar[5] had claimed that the strong solute−solvent interaction makes the NES effect negligible because the motion of solvent coupled with the solute strongly responds quickly to the solute reactive motion. The present findings, however, show that the motion of solvent strongly coupled to the solute is not necessarily fast compared with the solute reactive motion.

The force that the solvent exerts on the solute reactive motion will be important in the product region away from the TS because the IRP in this region is curved; this curve is caused by the change in the motion along the IRP from the solute reactive motion to the solvent reactive one. This retarding force, however, is expected to have a negligible effect *on the kinetics* of the microhydrated reactions because this region is close to the bottom of the energy barrier. Finally, it should be noted that the retarding force of the solvent, which arises in the product region, may influence the flow of energy from the energy-rich solute to the solution.

Concluding Remarks

We determined the IRP on the SRS for each of four reactions in the presence of two water molecules by carrying out ab initio calculations and showed that in the TS region the major component of the reaction-path motion is the solute reactive motion, whereas in the reactant and product regions the major component is the solvent reorganization. The rate-constant ratios k^{na}/k^{eq} and k^{TST}/k^{eq} were found to be nearly 1.0 for all the microhydrated reactions, irrespective of the strength of the solute−solvent interaction.

From these results for the four microhydrated reactions and the previous result for the CIP formation of *t*-BuCl in the presence of four water molecules, we can draw five conclusions: (1) The mechanism of solution reactions is a three-step mechanism whether the solute−solvent interaction is strong or weak. (2) The major role of solvent reorganization in the reaction occurrence is to reduce the activation barrier along the displacement of the solute reactive coordinate. (3) The solvent characterized as a frozen spectator in the IRP near the TS does not exert force on the solute reactive motion. (4) The strength of the NES effect cannot be determined by only the strength of the solute−solvent interaction. (5) The NES effect can be moderate if the solvent reactive motion is some component of the motion along the IRP in the TS region.

One can obtain significant insights into solution reactions by examining microsolvated systems including only a few solvent molecules even though the number of the solvent molecules in microsolvated systems may be too small to comprehensively model the multidimensional solvent space in actual solution reactions. Many studies have in fact shown that significant insights into solution reactions can be obtained by investigating microsolvated reactions. In the ionization of HCl in water, for example, the potential energy surface for a microhydrated system was shown by Ando and Hynes to be similar to that for the corresponding solution system.[30] Thus, the features noted in the present study should be qualitatively similar to those of actual solution reactions.

In the future, we will examine reactions in the presence of a large number of solvent molecules. This examination will give a more comprehensive understanding of the solution reactions. For this examination, the recent study of Gordon et al.[19,25] is encouraging because their method reduces the computational cost of treating such microsolvated reactions and still provides moderate accuracy.

Appendix: Reactive Coordinates at the Transition State

Although eqs 1 and 2 become indeterminate at the TS, the directions of the configuration changes attending the displacement of the solute and solvent reactive coordinates at the TS should be determined by the corresponding directions at any IRP point near the TS. At such a point, we have

$$\frac{\partial V}{\partial x_S^{\,i}} \approx \sum_{j=1}^{3N^S} \frac{\partial^2 V}{\partial x_S^{\,i}\,\partial x_S^{\,j}} \Delta x_S^{\,j} + \sum_{k=1}^{3N^B} \frac{\partial^2 V}{\partial x_S^{\,i}\,\partial x_B^{\,k}} \Delta x_B^{\,k} \qquad \text{(A1)}$$

and

$$\frac{\partial V}{\partial x_B^{\,l}} \approx \sum_{j=1}^{3N^S} \frac{\partial^2 V}{\partial x_B^{\,l}\,\partial x_S^{\,j}} \Delta x_S^{\,j} + \sum_{k=1}^{3N^B} \frac{\partial^2 V}{\partial x_B^{\,l}\,\partial x_B^{\,k}} \Delta x_B^{\,k} \qquad \text{(A2)}$$

where $\Delta x_S^{\,j}$ and $\Delta x_B^{\,k}$ are, respectively, the mass-weighted Cartesian displacements of solute and solvent from the TS. Then, according to eqs 1 and 2, the directions of the configuration changes attending the displacement of the solute and solvent reactive coordinates are given by

$$\frac{d\mathbf{x}_S}{ds^S} \approx A(\mathbf{F}_{SS}\Delta\mathbf{x}_S + \mathbf{F}_{SB}\Delta\mathbf{x}_B) \qquad \text{(A3)}$$

and

$$\frac{d\mathbf{x}_B}{ds^B} \approx B(\mathbf{F}_{BS}\Delta\mathbf{x}_S + \mathbf{F}_{BB}\Delta\mathbf{x}_B) \qquad \text{(A4)}$$

where A and B are constants, $\Delta\mathbf{x}_S \equiv \{\Delta x_S^{\,i}\}$, $\Delta\mathbf{x}_B \equiv \{\Delta x_B^{\,k}\}$,

$$\mathbf{F}_{SS} \equiv \left\{\frac{\partial^2 V}{\partial x_S^{\,i}\,\partial x_S^{\,j}}\right\},\ \mathbf{F}_{BB} \equiv \left\{\frac{\partial^2 V}{\partial x_B^{\,k}\,\partial x_B^{\,l}}\right\},\ \text{and}\ \mathbf{F}_{SB} = \mathbf{F}_{BS} \equiv \left\{\frac{\partial^2 V}{\partial x_S^{\,i}\,\partial x_B^{\,k}}\right\} \qquad \text{(A5)}$$

The direction tangential to the IRP is given by

$$\frac{d\mathbf{x}_S}{ds} \approx C(\mathbf{F}_{SS}\Delta\mathbf{x}_S + \mathbf{F}_{SB}\Delta\mathbf{x}_B) \qquad \text{(A6)}$$

and

(30) Ando, K.; Hynes, J. T. *J. Phys. Chem. B* **1997**, *101*, 10464−10478.

$$\frac{d\mathbf{x}_B}{ds} \approx C(\mathbf{F}_{BS}\Delta\mathbf{x}_S + \mathbf{F}_{BB}\Delta\mathbf{x}_B) \tag{A7}$$

where C is a constant. Thus we have

$$\frac{d\mathbf{x}}{ds} = \begin{bmatrix} \frac{C}{A}\frac{d\mathbf{x}_S}{ds^S} \\ \frac{C}{B}\frac{d\mathbf{x}_B}{ds^B} \end{bmatrix} \tag{A8}$$

The IRP tangent at the TS is obtained as the vector of the unstable normal mode whose vibrational frequency has an imaginary value.[11,31,32] Equation A8 therefore indicates that the directions tangential to the paths of the configuration changes attending the displacement of the solute and solvent reactive coordinates at the TS should coincide with the solute and solvent vectors in the unstable normal mode for the full solute−solvent space.

JA9940221

(31) Pechukas, P. *J. Chem. Phys.* **1976**, *64*, 1516−1521.
(32) Page, M.; McIver, J. W., Jr. *J. Chem. Phys.* **1988**, *88*, 922−935.